POG Modeling of a Cascaded Doubly-Fed Induction Generator

Roberto Zanasi
Information Engineering Department
University of Modena e Reggio Emilia
Via Vignolese 905
41100 Modena, Italy
Email: roberto.zanasi@unimore.it

Giovanni Azzone
Information Engineering Department
University of Modena e Reggio Emilia
Via Vignolese 905
41100 Modena, Italy
Email: giovanni.azzone@unimore.it

***Abstract*—In this paper a Cascaded Doubly-Fed Induction Generator (CDFIG) has been modeled using the Power-Oriented Graphs (POG) technique. The dynamic equations of the system have been obtained using a Lagrangian approach. The system equations have been described with respect to a rotating reference frame to clearly show the internal dynamic structure of the system. An Indirect Rotor Field-Oriented control that let the grid voltage frequency to be constant, even when the rotor speed is variable, has been given and implemented. Finally, some simulation results have been reported to validate the presented control law and the effectiveness of the model.**

I. Introduction

A CDFIG is a cascade of two wound rotor induction machines whose rotors are mechanically and electrically coupled, see Fig. 4: the stator of the M_2 motor is connected to the grid, while the stator of the M_1 motor is properly controlled. The CDFIG systems are widely used in renewable energy systems, like windmills or hydropower generators [1], as constant frequency power sources from variable speed prime movers. In [2] and [3] a CDFIG model is described, based on the inversion of the dynamical model of the system and using a dynamical equivalent circuit representation. In this paper the dynamic equations of the CDFIG system are obtained using a Lagrangian approach and the POG graphical technique: the obtained dynamic model is very compact and clear. The equations are referred to a rotating reference frame using an orthonormal state space transformation. A control law is implemented to ensure a constant grid frequency by modulating the controllable motor stator frequency. The paper is organized as follows: Sec. II describes the basic properties of the POG modeling technique. Sec. III shows the details of the CDFIG structure and the corresponding POG dynamic model. Finally, in Sec. IV some simulation results are reported.

II. Power-Oriented Graphs basic principles

The Power-Oriented Graphs technique, see [5], is suitable for modeling physical systems. The POG are normal block diagrams combined with a particular modular structure essentially based on the use of the two blocks shown in Fig. 1.a and Fig. 1.b: the *elaboration block* (e.b.) stores and/or dissipates energy (i.e. springs, masses, dampers, capacities, inductances, resistances, etc.); the *connection block* (c.b.) redistributes the

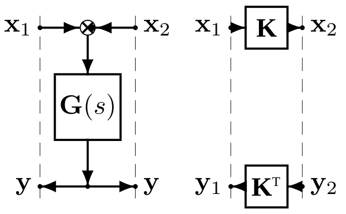

a) *e. b.* b) *c. b.*

	POG Variables	
Domains:	*Across:* v_e	*Through:* v_f
Electrical	Voltage V	Current I
Mec. Tra.	Velocity v	Force F
Mec. Rot.	Ang. Vel. ω	Torque τ
Hydraulic	Pressure P	Flow rate Q

c) *Across and through variables*

Figure 1. POG basic blocks and variables: a) *elaboration block*; b) *connection block*; c) *across and through variables*.

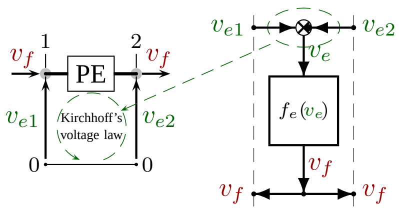

a) Element in series b) Inputs: v_{e1}, v_{e2}. c) Inputs: v_f, v_{e2}.

Figure 2. POG graphical representations of a Physical Element (PE) connected in series.

power within the system without storing nor dissipating energy (i.e. any type of gear reduction, transformers, etc.). The c.b. transforms the power variables with the constraint $\mathbf{x}_1^T\mathbf{y}_1 = \mathbf{x}_2^T\mathbf{y}_2$. The e.b. and the c.b. are suitable for representing both scalar and vectorial systems. In the vectorial case, $\mathbf{G}(s)$ and $\mathbf{K}$ are matrices: $\mathbf{G}(s)$ is a square matrix of positive definite functions, $\mathbf{K}$ can also be rectangular. The circle present in the e.b. is a summation element and the black spot represents a minus sign that multiplies the entering variable. The main feature of the Power-Oriented Graphs is to keep a direct correspondence between the dashed sections of the graphs and real power sections of the modeled systems: the scalar product $\mathbf{x}^T\mathbf{y}$ of the two *power vectors* $\mathbf{x}$ and $\mathbf{y}$ involved in each dashed line of a power-oriented graph, see Fig. 1, has the physical meaning of *the power flowing through that particular section*.

The main energetic domains encountered in modeling physical systems are the electrical, the mechanical (translational and rotational) and the hydraulic, see Fig. 1.c. Each energetic

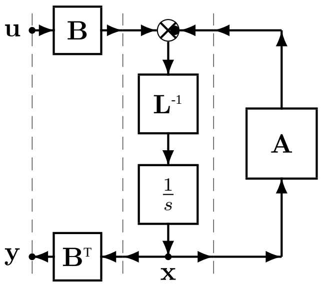

$$\begin{cases} \mathbf{L}\,\dot{\mathbf{x}} = -\mathbf{A}\mathbf{x} + \mathbf{B}\mathbf{u} \\ \mathbf{y} = \mathbf{B}^{\mathrm{T}}\mathbf{x} \end{cases} \qquad (1)$$

$$\Downarrow\ (\mathbf{x} = \mathbf{T}\mathbf{z})$$

$$\begin{cases} \overline{\mathbf{L}}\dot{\mathbf{z}} = -\overline{\mathbf{A}}\mathbf{z} + \overline{\mathbf{B}}\mathbf{u} \\ \mathbf{y} = \overline{\mathbf{B}}^{\mathrm{T}}\mathbf{z} \end{cases} \qquad (2)$$

Figure 3. POG block scheme of a generic dynamic system.

domain is characterized by two *power variables*: an *across-variable* v_e defined between two points (i.e. the voltage V), and a *through-variable* v_f defined in each point of the space (i.e. the current I). Each Physical Element (PE) interacts with the external world through the power sections associated to its terminals. A Physical Element is connected *in series* when its terminals share the same through-variable v_f, see Fig. 2.a. This physical element can be modeled using the POG block shown in Fig. 2.b: note that the summation element present in this block describes the Kirchhoff's law applied to the across-variables v_{e1}, v_{e2} and v_e. The physical element PE in Fig. 2.a can also be modeled using the POG block shown in Fig. 2.c. This is an "equivalent" *elaboration block* (with a different graphical shape) obtained from the POG block of Fig. 2.b inverting the path that goes from v_{e1} to v_f. Physical Elements connected *in parallel* share the same across-variable v_e. It can be easily shown that the POG modeling of the physical elements *in parallel* can be done in a way quite similar to the way used above for the elements *in series*. Another important aspect of the POG technique is the direct correspondence between the POG representations and the corresponding state space descriptions. For example, the POG scheme shown in Fig. 3 can be represented by the state space equations given in (1) where the *energy matrix* $\mathbf{L}$ is symmetric and positive definite: $\mathbf{L} = \mathbf{L}^{\mathrm{T}} > 0$. For such a system, the stored energy E_s and the dissipating power P_d can be expressed as follows: $E_s = \frac{1}{2}\mathbf{x}^{\mathrm{T}}\mathbf{L}\,\mathbf{x}$, $P_d = \mathbf{x}^{\mathrm{T}}\mathbf{A}\,\mathbf{x}$. When an eigenvalue of matrix $\mathbf{L}$ tends to zero (or to infinity), system (1) degenerates towards a lower dimension dynamic system. In this case, the dynamic model (2) of the "reduced" system can be directly obtained from (1) by using a simple "congruent" transformation $\mathbf{x} = \mathbf{T}\mathbf{z}$ ($\mathbf{T}$ is constant) where $\overline{\mathbf{L}} = \mathbf{T}^{\mathrm{T}}\mathbf{L}\mathbf{T}$, $\overline{\mathbf{A}} = \mathbf{T}^{\mathrm{T}}\mathbf{A}\mathbf{T}$ and $\overline{\mathbf{B}} = \mathbf{T}^{\mathrm{T}}\mathbf{B}$. If matrix $\mathbf{T}$ is time-varying, an additional term $\mathbf{T}^{\mathrm{T}}\mathbf{L}\dot{\mathbf{T}}\mathbf{z}$ appears in the transformed system. When matrix $\mathbf{T}$ is rectangular, the system is transformed and reduced at the same time.

A. Notations

In this paper the following notations are used:

- Column matrices:

$$\overset{i}{\underset{1:n}{[\![}}\, R_i \,]\!] = \left[\, R_1\ R_2 \cdots R_n \,\right]^{\mathrm{T}}.$$

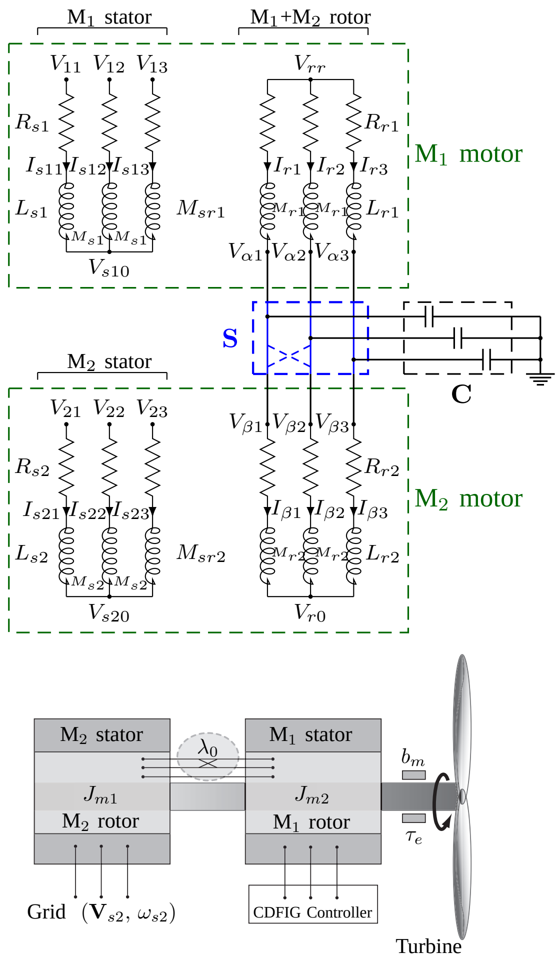

Figure 4. Electric scheme and structure of a CDFIG system.

- The symbols $\mathbf{j}$ and $e^{\mathbf{j}\theta}$ denote the following matrices:

$$\mathbf{j} = \begin{bmatrix} 0 & -1 \\ 1 & 0 \end{bmatrix}, \qquad e^{\mathbf{j}\theta} = \begin{bmatrix} \cos\theta & -\sin\theta \\ \sin\theta & \cos\theta \end{bmatrix}.$$

- The symbol $\mathbf{I}_m$ denotes an identity matrix of order m.

III. CDFIG Modeling

The structure and the electric scheme of a CDFIG system are shown in Fig. 4. The stator and rotor phases are star connected. This system in characterized by the parameters given in Tab. I where the subscript indices "$_1$" and "$_2$" refer to the motors M_1 and M_2, respectively. All the electric parameters of Tab. I have been obtained connecting in series the p_1 and p_2 polar couples of the two motors. Let ${}^t\mathbf{V}_{s1}$, ${}^t\mathbf{I}_{s1}$, ${}^t\mathbf{V}_{\alpha}$, ${}^t\mathbf{V}_{rr} = V_{rr}\,\mathbf{I}_3$, ${}^t\mathbf{I}_r$, ${}^t\mathbf{V}_{s2}$, ${}^t\mathbf{I}_{s2}$, ${}^t\mathbf{V}_{\beta}$, ${}^t\mathbf{V}_{r0} = V_{r0}\,\mathbf{I}_3$ and ${}^t\mathbf{I}_{\beta}$ denote the stator/rotor voltage and current vectors of the motors M_1 and M_2 in the original reference frame Σ_t:

$${}^t\mathbf{V}_{s1} = \begin{bmatrix} V_{s11} \\ V_{s12} \\ V_{s13} \end{bmatrix}, \quad {}^t\mathbf{I}_{s1} = \begin{bmatrix} I_{s11} \\ I_{s12} \\ I_{s13} \end{bmatrix}, \quad {}^t\mathbf{V}_{\alpha} = \begin{bmatrix} V_{\alpha 1} \\ V_{\alpha 2} \\ V_{\alpha 3} \end{bmatrix}, \quad {}^t\mathbf{I}_r = \begin{bmatrix} I_{r1} \\ I_{r2} \\ I_{r3} \end{bmatrix}$$

$p_1,\, p_2$	number of polar couples
γ	angular phase displacement ($\gamma = \frac{2\pi}{3}$)
θ_m	rotor angular position
ω_m	rotor angular velocity
$\theta_{s1},\, \theta_{s2}$	stator voltage angular positions
$\omega_{s1},\, \omega_{s2}$	stator voltage frequencies
$\theta_1,\, \theta_2$	electric angles ($\theta_1 = p_1\,\theta_m\ ,\ \theta_2 = p_2\,\theta_m$)
$\omega_1,\, \omega_2$	electric frequencies ($\omega_1 = p_1\,\omega_m\ ,\ \omega_2 = p_2\,\omega_m$)
$R_{s1},\, R_{s2}$	stator phase resistances
$L_{s1},\, L_{s2}$	stator phase self inductances
$M_{s10},\, M_{s20}$	stator phase mutual inductance maximum values
$R_{r1},\, R_{r2}$	rotor phase resistances
$L_{r1},\, L_{r2}$	rotor phase self inductances
$M_{r10},\, M_{r20}$	rotor phase mutual inductance maximum values
$M_{sr10},\, M_{sr20}$	stator/rotor phase mutual inductance maximum values
$J_{m1},\, J_{m2}$	rotor momentum inertia
$b_{m1},\, b_{m2}$	rotor linear friction coefficients
τ_m	electromotive torque acting on the rotor
τ_e	external load torque acting on the rotor

Table I
CDFIG SYSTEM PARAMETERS.

and

$$ {}^t\mathbf{V}_{s2} = \begin{bmatrix} V_{s21} \\ V_{s22} \\ V_{s23} \end{bmatrix},\ {}^t\mathbf{I}_{s2} = \begin{bmatrix} I_{s21} \\ I_{s22} \\ I_{s23} \end{bmatrix},\ {}^t\mathbf{V}_{\beta} = \begin{bmatrix} V_{\beta 1} \\ V_{\beta 2} \\ V_{\beta 3} \end{bmatrix},\ {}^t\mathbf{I}_{\beta} = \begin{bmatrix} I_{\beta 1} \\ I_{\beta 2} \\ I_{\beta 3} \end{bmatrix}. $$

where $V_{s1i} = V_{1i} - V_{s10}$ and $V_{s2i} = V_{2i} - V_{s20}$, see Fig. 4. All the possible rotor phase connections between the two motors can be described in a compact form by using the relation ${}^t\mathbf{V}_{\beta} = \mathbf{S}\,{}^t\mathbf{V}_{\alpha}$, see Fig. 4, where matrix $\mathbf{S}$ is defined as:

$$ \mathbf{S} = \begin{bmatrix} 1-\lambda_{12}-\lambda_{13} & \lambda_{12} & \lambda_{13} \\ \lambda_{12} & 1-\lambda_{12}-\lambda_{23} & \lambda_{23} \\ \lambda_{13} & \lambda_{23} & 1-\lambda_{13}-\lambda_{23} \end{bmatrix} $$

where $\lambda_{12},\, \lambda_{13},\, \lambda_{23} \in \{0, 1\}$ are binary variables satisfying the relation $\lambda_{12}+\lambda_{13}+\lambda_{23} \leq 1$. Only the four following rotor connections are possible:

$$ (\lambda_{12},\ \lambda_{13},\ \lambda_{23}) = \{(0\ 0\ 0),\ (1\ 0\ 0),\ (0\ 1\ 0),\ (0\ 0\ 1)\}\,. $$

Matrix $\mathbf{S}$ satisfies the following properties:

$$ \mathbf{S}^{\text{-1}} = \mathbf{S}^{\text{T}} = \mathbf{S}^{\text{-T}} = \mathbf{S}, \qquad \mathbf{S}^2 = \mathbf{S}^{\text{T}}\mathbf{S} = \mathbf{S}\mathbf{S}^{\text{T}} = \mathbf{I}_3. \qquad (3) $$

Connecting the two rotors using the $\mathbf{S}$ matrix and adding the fictitious capacitors $\mathbf{C} = C\,\mathbf{I}_3$ to terminals $V_{\alpha 1}$, $V_{\alpha 2}$ and $V_{\alpha 3}$, see Fig. 4, one obtains the following dynamic equations of the electrical part of CDFIG system:

$$ \begin{aligned} &\frac{d}{dt}\Bigg(\underbrace{\begin{bmatrix} {}^t\mathbf{L}_{s1} & {}^t\mathbf{M}^{\text{T}}_{sr1} & 0 & 0 & 0 \\ {}^t\mathbf{M}_{sr1} & {}^t\mathbf{L}_{r1} & 0 & 0 & 0 \\ 0 & 0 & \mathbf{C} & 0 & 0 \\ 0 & 0 & 0 & {}^t\mathbf{L}_{r2} & {}^t\mathbf{M}^{\text{T}}_{sr2} \\ 0 & 0 & 0 & {}^t\mathbf{M}_{sr2} & {}^t\mathbf{L}_{s2} \end{bmatrix}}_{{}^0\mathbf{L}_e} \underbrace{\begin{bmatrix} {}^t\mathbf{I}_{s1} \\ {}^t\mathbf{I}_{r} \\ {}^t\mathbf{V}_{\alpha} \\ {}^t\mathbf{I}_{\beta} \\ {}^t\mathbf{I}_{s2} \end{bmatrix}}_{{}^0\mathbf{q}_e}\Bigg) = \\ &= \underbrace{\begin{bmatrix} -{}^t\mathbf{R}_{s1} & 0 & 0 & 0 & 0 \\ 0 & -{}^t\mathbf{R}_{r1} & -\mathbf{I}_3 & 0 & 0 \\ 0 & \mathbf{I}_3 & 0 & -\mathbf{S}^{\text{T}} & 0 \\ 0 & 0 & \mathbf{S} & -{}^t\mathbf{R}_{r2} & 0 \\ 0 & 0 & 0 & 0 & -{}^t\mathbf{R}_{s2} \end{bmatrix}}_{{}^0\mathbf{R}_e} \underbrace{\begin{bmatrix} {}^t\mathbf{I}_{s1} \\ {}^t\mathbf{I}_{r} \\ {}^t\mathbf{V}_{\alpha} \\ {}^t\mathbf{I}_{\beta} \\ {}^t\mathbf{I}_{s2} \end{bmatrix}}_{{}^0\mathbf{q}_e} + \underbrace{\begin{bmatrix} {}^t\mathbf{V}_{s1} \\ {}^t\mathbf{V}_{rr} \\ 0 \\ -{}^t\mathbf{V}_{r0} \\ {}^t\mathbf{V}_{s2} \end{bmatrix}}_{{}^0\mathbf{V}_e} \end{aligned} \qquad (4) $$

where:

$$ {}^t\mathbf{L}_{s1} = \begin{bmatrix} L_{s1} & -\frac{M_{s10}}{2} & -\frac{M_{s10}}{2} \\ -\frac{M_{s10}}{2} & L_{s1} & -\frac{M_{s10}}{2} \\ -\frac{M_{s10}}{2} & -\frac{M_{s10}}{2} & L_{s1} \end{bmatrix},\quad {}^t\mathbf{L}_{r1} = \begin{bmatrix} L_{r1} & -\frac{M_{r10}}{2} & -\frac{M_{r10}}{2} \\ -\frac{M_{r10}}{2} & L_{r1} & -\frac{M_{r10}}{2} \\ -\frac{M_{r10}}{2} & -\frac{M_{r10}}{2} & L_{r1} \end{bmatrix}, $$

$$ {}^t\mathbf{L}_{s2} = \begin{bmatrix} L_{s2} & -\frac{M_{s20}}{2} & -\frac{M_{s20}}{2} \\ -\frac{M_{s20}}{2} & L_{s2} & -\frac{M_{s20}}{2} \\ -\frac{M_{s20}}{2} & -\frac{M_{s20}}{2} & L_{s2} \end{bmatrix},\quad {}^t\mathbf{L}_{r2} = \begin{bmatrix} L_{r2} & -\frac{M_{r20}}{2} & -\frac{M_{r20}}{2} \\ -\frac{M_{r20}}{2} & L_{s2} & -\frac{M_{r20}}{2} \\ -\frac{M_{r20}}{2} & -\frac{M_{r20}}{2} & L_{s2} \end{bmatrix}, $$

$$ {}^t\mathbf{M}_{sr1}(\theta_m) = M_{sr10} \begin{bmatrix} \cos(\theta_1) & \cos(\theta_1-\gamma) & \cos(\theta_1-2\gamma) \\ \cos(\theta_1+\gamma) & \cos(\theta_1) & \cos(\theta_1-\gamma) \\ \cos(\theta_1+2\gamma) & \cos(\theta_1+\gamma) & \cos(\theta_1) \end{bmatrix}, $$

$$ {}^t\mathbf{M}_{sr2}(\theta_m) = M_{sr20} \begin{bmatrix} \cos(\theta_2) & \cos(\theta_2+\gamma) & \cos(\theta_2+2\gamma) \\ \cos(\theta_2-\gamma) & \cos(\theta_2) & \cos(\theta_2+\gamma) \\ \cos(\theta_2-2\gamma) & \cos(\theta_2-\gamma) & \cos(\theta_2) \end{bmatrix}, $$

$$ {}^t\mathbf{R}_{s1} = R_{s1}\mathbf{I}_3,\ \ {}^t\mathbf{R}_{r1} = R_{r1}\mathbf{I}_3,\ \ {}^t\mathbf{R}_{s2} = R_{s2}\mathbf{I}_3,\ \ {}^t\mathbf{R}_{r2} = R_{r2}\mathbf{I}_3. $$

When in (4) the capacitors tend to zero, $\mathbf{C} \to 0$, one obtains the static relation ${}^t\mathbf{I}_{\beta} = \mathbf{S}^{\text{-T}}\,{}^t\mathbf{I}_r$ between the two rotor current vectors. Applying the following rectangular transformation ${}^0\mathbf{q}_e = {}^0\mathbf{T}_t\ {}^t\mathbf{I}_e$ to system (4) (note that from (3) it is $\mathbf{S}^{\text{-T}} = \mathbf{S}$):

$$ {}^0\mathbf{T}_t = \begin{bmatrix} \mathbf{I}_3 & 0 & 0 \\ 0 & \mathbf{I}_3 & 0 \\ 0 & 0 & 0 \\ 0 & \mathbf{S}^{\text{-T}} & 0 \\ 0 & 0 & \mathbf{I}_3 \end{bmatrix} = \begin{bmatrix} \mathbf{I}_3 & 0 & 0 \\ 0 & \mathbf{I}_3 & 0 \\ 0 & 0 & 0 \\ 0 & \mathbf{S} & 0 \\ 0 & 0 & \mathbf{I}_3 \end{bmatrix} $$

one obtains the following reduced dynamic equations:

$$ \begin{aligned} &\frac{d}{dt}\Bigg(\underbrace{\begin{bmatrix} {}^t\mathbf{L}_{s1} & {}^t\mathbf{M}^{\text{T}}_{sr1}(\theta_m) & 0 \\ {}^t\mathbf{M}_{sr1}(\theta_m) & {}^t\mathbf{L}_{r} & \mathbf{S}^{\text{T}}\,{}^t\mathbf{M}^{\text{T}}_{sr2}(\theta_m) \\ 0 & {}^t\mathbf{M}_{sr2}(\theta_m)\mathbf{S} & {}^t\mathbf{L}_{s2} \end{bmatrix}}_{{}^t\mathbf{L}_e} \underbrace{\begin{bmatrix} {}^t\mathbf{I}_{s1} \\ {}^t\mathbf{I}_{r} \\ {}^t\mathbf{I}_{s2} \end{bmatrix}}_{{}^t\mathbf{I}_e}\Bigg) = \\ &= -\underbrace{\begin{bmatrix} {}^t\mathbf{R}_{s1} & 0 & 0 \\ 0 & {}^t\mathbf{R}_{r} & 0 \\ 0 & 0 & {}^t\mathbf{R}_{s2} \end{bmatrix}}_{{}^t\mathbf{R}_e} \underbrace{\begin{bmatrix} {}^t\mathbf{I}_{s1} \\ {}^t\mathbf{I}_{r} \\ {}^t\mathbf{I}_{s2} \end{bmatrix}}_{{}^t\mathbf{I}_e} + \underbrace{\begin{bmatrix} {}^t\mathbf{V}_{s1} \\ {}^t\mathbf{V}_{r} \\ {}^t\mathbf{V}_{s2} \end{bmatrix}}_{{}^t\mathbf{V}_e} \end{aligned} \qquad (5) $$

In compact form it can be expressed as:

$$ \frac{d}{dt}\left({}^t\mathbf{L}_e\ {}^t\mathbf{I}_e\right) = -\,{}^t\mathbf{R}_e\ {}^t\mathbf{I}_e + {}^t\mathbf{V}_e \qquad (6) $$

where ${}^t\mathbf{L}_r = {}^t\mathbf{L}_{r1} + {}^t\mathbf{L}_{r2}$, ${}^t\mathbf{R}_r = {}^t\mathbf{R}_{r1} + {}^t\mathbf{R}_{r2}$ and ${}^t\mathbf{V}_r = {}^t\mathbf{V}_{rr} - \mathbf{S}^{\text{T}}\,{}^t\mathbf{V}_{r0} = 0$. Let us now define the following generalized state vectors ${}^t\mathbf{q}$, ${}^t\dot{\mathbf{q}}$ and extended input vector ${}^t\mathbf{V}$:

$$ {}^t\mathbf{q} = \begin{bmatrix} {}^t\mathbf{Q}_{s1} \\ {}^t\mathbf{Q}_{r} \\ {}^t\mathbf{Q}_{s2} \\ \hline \theta_m \end{bmatrix},\qquad {}^t\dot{\mathbf{q}} = \begin{bmatrix} {}^t\mathbf{I}_e \\ \omega_m \end{bmatrix},\qquad {}^t\mathbf{V} = \begin{bmatrix} {}^t\mathbf{V}_e \\ -\tau_e \end{bmatrix}. $$

Let ${}^t\mathbf{L}({}^t\mathbf{q})$ and ${}^t\mathbf{R}$ denote the following matrices:

$$ {}^t\mathbf{L}({}^t\mathbf{q}) = \begin{bmatrix} {}^t\mathbf{L}_e & 0 \\ 0 & J_m \end{bmatrix},\qquad {}^t\mathbf{R} = \begin{bmatrix} {}^t\mathbf{R}_e & 0 \\ 0 & b_m \end{bmatrix} $$

where $J_m = J_{m1} + J_{m2}$ and $b_m = b_{m1} + b_{m2}$. Using a Lagrangian approach, see [6] and [7], the dynamic equations of the full CDFIG system can be expressed as:

$$ \frac{d}{dt}\left(\frac{\partial K}{\partial\,{}^t\dot{\mathbf{q}}^{\text{T}}}\right) - \frac{\partial K}{\partial\,{}^t\mathbf{q}^{\text{T}}} = {}^t\mathbf{V} - {}^t\mathbf{R}\,{}^t\dot{\mathbf{q}} \qquad (7) $$

where the Lagrangian function $K({}^t\mathbf{q},\,{}^t\dot{\mathbf{q}})$ is defined as:

$$K(\,{}^t\mathbf{q},\,{}^t\dot{\mathbf{q}})\,{}^t\dot{\mathbf{q}} = \frac{1}{2}\,{}^t\dot{\mathbf{q}}^{\mathrm{T}}\,{}^t\mathbf{L}({}^t\mathbf{q})\,{}^t\dot{\mathbf{q}}\,. \tag{8}$$

From (7) and (8) one obtains the CDFIG dynamic equations:

$$\frac{d}{dt}\Bigg(\underbrace{\left[\begin{array}{c|c} {}^t\mathbf{L}_e & 0 \\ \hline 0 & J_m \end{array}\right]}_{{}^t\mathbf{L}({}^t\mathbf{q})}\underbrace{\left[\begin{array}{c} {}^t\mathbf{I}_e \\ \hline \omega_m \end{array}\right]}_{{}^t\dot{\mathbf{q}}}\Bigg) = -\underbrace{\left[\begin{array}{c|c} {}^t\mathbf{R}_e + {}^t\mathbf{F}_e & {}^t\mathbf{K}_e \\ \hline -\,{}^t\mathbf{K}_e^{\mathrm{T}} & b_m \end{array}\right]}_{{}^t\mathbf{R}+\,{}^t\mathbf{W}}\underbrace{\left[\begin{array}{c} {}^t\mathbf{I}_e \\ \hline \omega_m \end{array}\right]}_{{}^t\dot{\mathbf{q}}} + \underbrace{\left[\begin{array}{c} {}^t\mathbf{V}_e \\ \hline -\tau_e \end{array}\right]}_{{}^t\mathbf{V}} \tag{9}$$

that in compact form can be expressed as:

$$\frac{d}{dt}\left({}^t\mathbf{L}\;{}^t\dot{\mathbf{q}}\right) = -({}^t\mathbf{R} + {}^t\mathbf{W})\,{}^t\dot{\mathbf{q}} + {}^t\mathbf{V} \tag{10}$$

where matrix ${}^t\mathbf{W}$ has the following structure:

$${}^t\mathbf{W} = \left[\begin{array}{ccc|c} 0 & -\frac{1}{2}\,{}^t\dot{\mathbf{M}}_{sr1}^{\mathrm{T}} & 0 & {}^t\mathbf{K}_{s1} \\ -\frac{1}{2}\,{}^t\dot{\mathbf{M}}_{sr1} & 0 & -\frac{1}{2}\mathbf{S}^{\mathrm{T}}\,{}^t\dot{\mathbf{M}}_{sr2}^{\mathrm{T}} & {}^t\mathbf{K}_r \\ 0 & -\frac{1}{2}\,{}^t\dot{\mathbf{M}}_{sr2}\mathbf{S} & 0 & {}^t\mathbf{K}_{s2} \\ \hline -\,{}^t\mathbf{K}_{s1}^{\mathrm{T}} & -\,{}^t\mathbf{K}_r^{\mathrm{T}} & -\,{}^t\mathbf{K}_{s2}^{\mathrm{T}} & 0 \end{array}\right]$$

Matrix ${}^t\mathbf{W}$ is skew-symmetric: ${}^t\mathbf{W}^{\mathrm{T}} = -\,{}^t\mathbf{W}$. The components of the torque vector ${}^t\mathbf{K}_e^{\mathrm{T}} = \left[\,{}^t\mathbf{K}_{s1}^{\mathrm{T}}\;{}^t\mathbf{K}_r^{\mathrm{T}}\;{}^t\mathbf{K}_{s2}^{\mathrm{T}}\right]$ are:

$${}^t\mathbf{K}_{s1}^{\mathrm{T}} = \frac{1}{2}\,{}^t\mathbf{I}_r^{\mathrm{T}}\frac{\partial\,{}^t\mathbf{M}_{sr1}(\theta_m)}{\partial\theta_m}, \quad {}^t\mathbf{K}_{s2}^{\mathrm{T}} = \frac{1}{2}\,{}^t\mathbf{I}_r^{\mathrm{T}}\,\mathbf{S}^{\mathrm{T}}\frac{\partial\,{}^t\mathbf{M}_{sr2}^{\mathrm{T}}(\theta_m)}{\partial\theta_m},$$

$${}^t\mathbf{K}_r^{\mathrm{T}} = \frac{1}{2}\,{}^t\mathbf{I}_{s1}^{\mathrm{T}}\frac{\partial\,{}^t\mathbf{M}_{sr1}^{\mathrm{T}}(\theta_m)}{\partial\theta_m} + \frac{1}{2}\,{}^t\mathbf{I}_{s2}^{\mathrm{T}}\frac{\partial\,{}^t\mathbf{M}_{sr2}(\theta_m)}{\partial\theta_m}\mathbf{S}.$$

Using the following rectangular matrix:

$${}^t\overline{\mathbf{T}}_\omega(\theta) = \sqrt{\frac{2}{3}}\;\underset{0:2}{\overset{h}{[\![}}\cos(h\,\gamma - \theta)\;,\;\sin(h\,\gamma - \theta)\,]\!]$$

one can define the orthonormal transformation matrix ${}^t\tilde{\mathbf{T}}_\omega$ as:

$${}^t\tilde{\mathbf{T}}_\omega = \begin{bmatrix} {}^t\overline{\mathbf{T}}_\omega(\theta_{s1}) & 0 & 0 \\ 0 & {}^t\overline{\mathbf{T}}_\omega(\theta_{s1}-\theta_1) & 0 \\ 0 & 0 & {}^t\overline{\mathbf{T}}_\omega(\lambda_0\,(\theta_{s1}-\theta_1-\gamma_1)+\theta_2) \end{bmatrix}$$

where $\lambda_0 = 1\text{–}2(\lambda_{12}+\lambda_{13}+\lambda_{23})$ and $\gamma_1 = (\lambda_{12}-\lambda_{13})\gamma$. Matrix ${}^t\tilde{\mathbf{T}}_\omega$ represents a multiple rotation in the state space which transforms the system variables from the original reference frame Σ_t to the rotating frame Σ_ω. The dynamic equations in the new transformed frame Σ_ω become:

$$\underbrace{\left[\begin{array}{c|c} {}^\omega\mathbf{L}_e & 0 \\ \hline 0 & J_m \end{array}\right]}_{{}^\omega\mathbf{L}}\underbrace{\left[\begin{array}{c} {}^\omega\dot{\mathbf{I}}_e \\ \hline \dot{\omega}_m \end{array}\right]}_{{}^\omega\ddot{\mathbf{q}}} = -\underbrace{\left[\begin{array}{c|c} {}^\omega\mathbf{R}_e + {}^\omega\mathbf{F}_e + {}^\omega\mathbf{\Omega}_e & {}^\omega\mathbf{K}_e \\ \hline -\,{}^\omega\mathbf{K}_e^{\mathrm{T}} & b_m \end{array}\right]}_{{}^\omega\mathbf{R}+\,{}^\omega\mathbf{W}}\underbrace{\left[\begin{array}{c} {}^\omega\mathbf{I}_e \\ \hline \omega_m \end{array}\right]}_{{}^\omega\dot{\mathbf{q}}} + \underbrace{\left[\begin{array}{c} {}^\omega\mathbf{V}_e \\ \hline -\tau_e \end{array}\right]}_{{}^\omega\mathbf{V}}$$

that in compact form can be expressed as:

$${}^\omega\mathbf{L}\;{}^\omega\ddot{\mathbf{q}} = -({}^\omega\mathbf{R} + {}^\omega\mathbf{W})\;{}^\omega\dot{\mathbf{q}} + {}^\omega\mathbf{V} \tag{11}$$

where ${}^\omega\mathbf{L} = {}^t\mathbf{T}_\omega^{\mathrm{T}}\,{}^t\mathbf{L}\,{}^t\mathbf{T}_\omega$, ${}^\omega\mathbf{R} = {}^t\mathbf{T}_\omega^{\mathrm{T}}\,{}^t\mathbf{R}\,{}^t\mathbf{T}_\omega = {}^t\mathbf{R}$, ${}^\omega\mathbf{W} = {}^t\mathbf{T}_\omega^{\mathrm{T}}\,{}^t\mathbf{W}\,{}^t\mathbf{T}_\omega$, ${}^\omega\mathbf{V} = {}^t\mathbf{T}_\omega^{\mathrm{T}}\,{}^t\mathbf{V}$, ${}^\omega\mathbf{K}_e^{\mathrm{T}} = {}^t\mathbf{T}_\omega^{\mathrm{T}}\,{}^t\mathbf{K}_e^{\mathrm{T}}$, ${}^\omega\dot{\mathbf{q}} = {}^t\mathbf{T}_\omega^{\mathrm{T}}\,{}^t\dot{\mathbf{q}}$ and matrix ${}^t\mathbf{T}_\omega$ has the following structure:

$${}^t\mathbf{T}_\omega = \left[\begin{array}{c|c} {}^t\tilde{\mathbf{T}}_\omega & 0 \\ \hline 0 & 1 \end{array}\right].$$

A POG graphical representation of system (11) is shown in Fig. 5. Note that the two terms ${}^\omega\mathbf{K}_e\,\omega_m$ and ${}^\omega\mathbf{F}_e\,{}^\omega\mathbf{I}_e$ have no effects on the system dynamics because it can be shown that ${}^\omega\mathbf{F}_e\,{}^\omega\mathbf{I}_e = -\,{}^\omega\mathbf{K}_e\,\omega_m$ and therefore they simplify each other. The expanded form of system (11) is given in Fig. 6, Eq. 13 where:

$$\omega_{p1} = \omega_{s1} - \omega_1, \qquad \omega_{s2} = \lambda_0(\omega_{s1}-\omega_1)+\omega_2$$

and:

$$L_{s1e} = L_{s10} + \tfrac{3}{2}M_{s10}, \qquad L_{s2e} = L_{s20} + \tfrac{3}{2}M_{s20},$$
$$M_{sr1e} = \tfrac{3}{2}\,M_{sr10}, \qquad M_{sr2e} = \tfrac{3}{2}\,M_{sr20},$$
$$L_{re} = L_{r0} + \tfrac{3}{2}M_{r0}, \qquad \mathbf{\Lambda} = \begin{bmatrix} 1 & 0 \\ 0 & \lambda_0 \end{bmatrix}.$$

Matrix $\mathbf{\Lambda}$ satisfies the following properties:

$$\begin{aligned} \mathbf{\Lambda}\,e^{\mathbf{j}\,\varphi} &= e^{\mathbf{j}\,\lambda_0\varphi}\mathbf{\Lambda}, & e^{\mathbf{j}\,\varphi}\mathbf{\Lambda} &= \mathbf{\Lambda}\,e^{\mathbf{j}\,\lambda_0\varphi}, \\ \mathbf{\Lambda}\,\mathbf{j} &= \lambda_0\,\mathbf{j}\,\mathbf{\Lambda}, & \mathbf{j}\,\mathbf{\Lambda} &= \lambda_0\,\mathbf{\Lambda}\,\mathbf{j}\,. \end{aligned} \tag{12}$$

Fig. 6 shows that the energy matrix ${}^\omega\mathbf{L}$ is now constant. The mechanical torque τ_m in the Σ_ω rotating frame can now be expressed as follows:

$$\begin{aligned} \tau_m &= {}^\omega\mathbf{K}_e^{\mathrm{T}}\,{}^\omega\mathbf{I}_e = \left[\,{}^\omega\mathbf{K}_{s1}^{\mathrm{T}}\;{}^\omega\mathbf{K}_r^{\mathrm{T}}\;{}^\omega\mathbf{K}_{s2}^{\mathrm{T}}\right]\begin{bmatrix} {}^\omega\mathbf{I}_{s1} \\ {}^\omega\mathbf{I}_r \\ {}^\omega\mathbf{I}_{s2} \end{bmatrix} \\ &= \begin{bmatrix} -\frac{1}{2}\,p_1\,M_{sr1e}\,{}^\omega\mathbf{I}_r^{\mathrm{T}}\,\mathbf{j} \\ \frac{1}{2}\,p_1\,M_{sr1e}\,{}^\omega\mathbf{I}_{s1}^{\mathrm{T}}\,\mathbf{j} + \frac{1}{2}\,p_2\,M_{sr2e}\,{}^\omega\mathbf{I}_{s2}^{\mathrm{T}}\,\mathbf{j}\,\mathbf{\Lambda} \\ -\frac{1}{2}\,p_2\,M_{sr2e}\,{}^\omega\mathbf{I}_r^{\mathrm{T}}\,\mathbf{\Lambda}\,\mathbf{j} \end{bmatrix}^{\mathrm{T}}\begin{bmatrix} {}^\omega\mathbf{I}_{s1} \\ {}^\omega\mathbf{I}_r \\ {}^\omega\mathbf{I}_{s2} \end{bmatrix} \\ &= p_1\,M_{sr1e}\,{}^\omega\mathbf{I}_{s1}^{\mathrm{T}}\,\mathbf{j}\,{}^\omega\mathbf{I}_r + p_2\,M_{sr2e}\,{}^\omega\mathbf{I}_{s2}^{\mathrm{T}}\,\mathbf{j}\,\mathbf{\Lambda}\,{}^\omega\mathbf{I}_r\,. \end{aligned}$$

An Indirect Rotor Field-Oriented control (IRFO), see [8], has been implemented for the M_1 motor obtaining:

$$\tau_m = \frac{p_1\,M_{sr1e}}{L_{re}}\,{}^\omega\Phi_{rd}\,{}^\omega I_{s1q} = \frac{{}^\omega\Phi_{rd}\,{}^\omega I_{s1q}}{K_\tau} \tag{14}$$

where ${}^\omega\Phi_{rd}$ is the direct component of the rotor flux:

$${}^\omega\Phi_{rd} = M_{sr1e}\,{}^\omega I_{s1d} = \frac{{}^\omega I_{s1d}}{K_\phi} \tag{15}$$

and:

$$\omega_{p1} = \frac{{}^\omega I_{s1q}}{T_r\,{}^\omega I_{s1d}} \tag{16}$$

Parameter $T_r = L_{re}/R_r$ is the rotor constant and the subscript indices "$_d$" and "$_q$" refer to the direct and quadrature vector components. The implemented IRFO control scheme is shown in Fig. 7: the PI_1 regulator controls the angular velocity ω_m, generating a torque reference τ_m^{ref} by tracking the following speed reference:

$$\omega_m^{ref} = \frac{\omega_{s2}^{des}}{p_2} - \frac{\omega_{p1}}{\lambda_0\,p_2} \tag{17}$$

where ω_{s2}^{des} is the desired output frequency. The PI_2 and PI_3 controllers regulate the mechanical torque τ_m and the rotor flux component ${}^\omega\Phi_{rd}$ respectively, according to the equations (14) and (15), generating the voltage references ${}^\omega V_{s1d}^{ref}$ and ${}^\omega V_{s1q}^{ref}$ for the motor M_1. The slip frequency ω_{p1} is calculated using the current references ${}^\omega I_{s1d}^{ref}$ and ${}^\omega I_{s1q}^{ref}$, see (16).

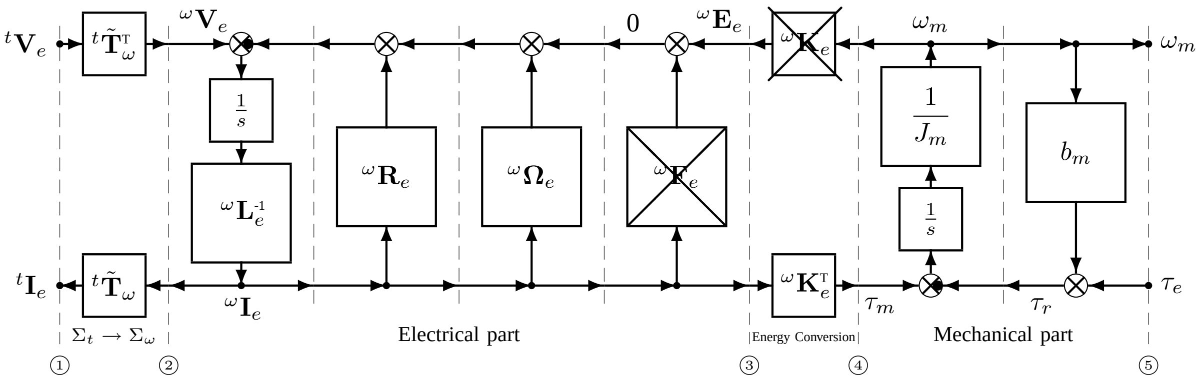

Figure 5. POG graphical representation of the CDFIG system in the transformed rotating reference frame Σ_ω.

$$\underbrace{\left[\begin{array}{ccc|c} L_{s1e}\,\mathbf{I}_2 & M_{sr1e}\,\mathbf{I}_2 & 0 & 0\\ M_{sr1e}\,\mathbf{I}_2 & L_{re}\,\mathbf{I}_2 & \mathbf{\Lambda} M_{sr2e} & 0\\ 0 & M_{sr2e}\,\mathbf{\Lambda} & L_{s2e}\,\mathbf{I}_2 & 0\\ \hline 0 & 0 & 0 & J_m \end{array}\right]}_{^\omega\mathbf{L}} \underbrace{\left[\begin{array}{c} ^\omega\dot{\mathbf{I}}_{s1}\\ ^\omega\dot{\mathbf{I}}_{r}\\ ^\omega\dot{\mathbf{I}}_{s2}\\ \hline \dot{\omega}_m \end{array}\right]}_{^\omega\dot{\mathbf{q}}} = - \underbrace{\left[\begin{array}{ccc|c} R_{s1}\mathbf{I}_2+\omega_{s1}\,L_{s1e}\,\mathbf{j} & \omega_{s1}\,M_{sr1e}\,\mathbf{j} & 0 & 0\\ \omega_{p1}\,M_{sr1e}\,\mathbf{j} & R_r\mathbf{I}_2+\omega_{p1}\,L_{re}\,\mathbf{j} & \omega_{p1}\,M_{sr2e}\,\mathbf{j}\,\mathbf{\Lambda} & 0\\ 0 & \omega_{s2}\,M_{sr2e}\,\mathbf{j}\,\mathbf{\Lambda} & R_{s2}\mathbf{I}_2+\omega_{s2}\,L_{s2e}\,\mathbf{j} & 0\\ \hline -\,^\omega\mathbf{K}_{s1}^{\mathrm{T}} & -\,^\omega\mathbf{K}_{r}^{\mathrm{T}} & -\,^\omega\mathbf{K}_{s2}^{\mathrm{T}} & b_m \end{array}\right]}_{^\omega\mathbf{R}+\,^\omega\mathbf{W}} \underbrace{\left[\begin{array}{c} ^\omega\mathbf{I}_{s1}\\ ^\omega\mathbf{I}_{r}\\ ^\omega\mathbf{I}_{s2}\\ \hline \omega_m \end{array}\right]}_{^\omega\mathbf{q}} + \underbrace{\left[\begin{array}{c} ^\omega\mathbf{V}_{s1}\\ 0\\ ^\omega\mathbf{V}_{s2}\\ \hline -\tau_e \end{array}\right]}_{^\omega\mathbf{V}} \qquad (13)$$

Figure 6. Dynamic equations of the CDFIG system in the transformed rotating reference frame Σ_ω.

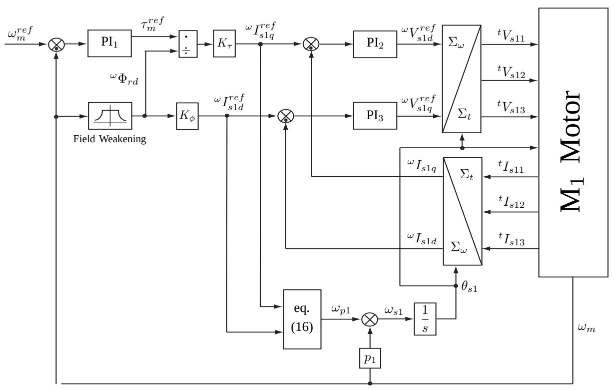

Figure 7. Indirect Rotor Field-Oriented control scheme implemented for the motor M_1.

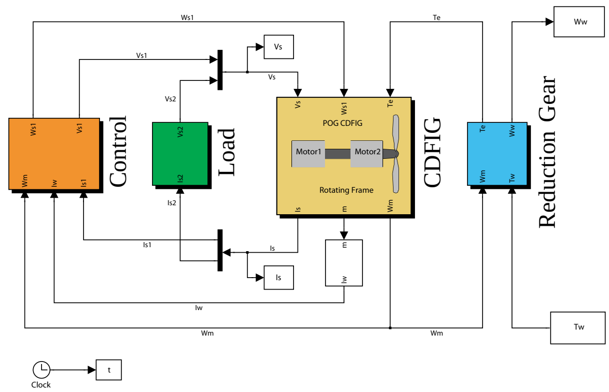

Figure 8. Simulink block scheme of a CDFIG system.

IV. Simulation results

The Matlab/Simulink block scheme corresponding to the obtained dynamic model of the CDFIG system is shown in Fig. 8. An additional Reduction Gear (reduction ratio ρ) has been introduced to connect the CDFIG system with the external turbine. The Load is composed, for each phase, by the parallel of a C_{load} capacity and a R_{load} resistance. The Control block implements the Indirect Rotor Field-Oriented control described in the previous section. The simulation results presented in this section have been obtained using the parameters shown in Tab. II. The motor M_1 is supplied by balanced voltages $V_{s1k} = V_{max}\cos(\omega_{s1}t-(k-1)\gamma)$, where $k \in \{1,\,2,\,3\}$ and $V_{max} = 100$ V. A constant external torque $\tau_w = 300$ Nm has been applied to the turbine. In Fig. 9 the stator voltage vectors of the M_1 and M_2 motors in the range $t \in [0.6,\;1.2]$ s are shown: $^t\mathbf{V}_{s1}$ evolves with a decreasing frequency according to the behavior of the frequency ω_{s1} reported in Fig. 10, whereas $^t\mathbf{V}_{s2}$ settles to a steady-state value with the constant frequency ω_{s2}^{des} imposed by (17). The second picture of Fig. 10 shows the negative mechanical torque τ_m absorbed by the generator and used to produce on the grid the output electric power. Fig. 11 shows the time behaviors of the stator and rotor current vectors $^t\mathbf{I}_{s1}$, $^t\mathbf{I}_r$ and $^t\mathbf{I}_{s2}$ in the range $t \in [0.6,\;1.2]$ s. Finally, Fig. 12 shows the desired (dotted black) and the actual (solid blue) time behaviors of ω_m, $^\omega I_{s1d}$ and $^\omega I_{s1q}$ in the range $t \in [0.6,\;1.5]$ s: the angular velocity ω_m perfectly overlaps his reference, while the $^\omega I_{s1d}$ and $^\omega I_{s1q}$ components settles to their steady-state values after a brief transient.

V. Conclusions

In this paper a Cascaded Doubly-Fed Induction Generator has been modeled using the POG technique and the dynamic equations have been obtained using a Lagrangian approach:

$\mathbf{M}_1$ **motor**	$\mathbf{M}_2$ **motor**
$p_1 = 1$	$p_2 = 1$
$L_{s1} = 135$ mH	$L_{s2} = 290$ mH
$M_{s10} = 20.3$ mH	$M_{s20} = 23.2$ mH
$R_{s1} = 0.9\,\Omega$	$R_{s2} = 1.8\,\Omega$
$L_{r1} = 19$ mH	$L_{r2} = 20$ mH
$M_{r10} = 2.8$ mH	$M_{r20} = 1.6$ mH
$R_{r1} = 1\,\Omega$	$R_{r2} = 0.5\,\Omega$
$M_{sr10} = 32$ mH	$M_{sr20} = 50$ mH
$J_{m1} = 0.1$ Kg m^2	$J_{m2} = 0.1$ Kg m^2
$b_{m1} = 0.1$ Nm s/rad	$b_{m2} = 0.1$ Nm s/rad
Rotor connection parameters	
$\lambda_{12} = \lambda_{13} = 0$, $\lambda_{23} = 1$	
Linear Load	
$C_{load} = 1\,\mu$F, $R_{load} = 50\,\Omega$	
Desired output frequency	
$\omega_{s2}^{des} = 2\pi\, F_{grid}$, $F_{grid} = 50$ Hz	
Turbine and Reduction gear parameters	
$J_t = 1.2$ Kg m^2, $b_t = 0.3$ Nm s/rad	
$\tau_w = 300$ Nm, $\rho = 5$	

Table II
CDFIG MODEL PARAMETERS.

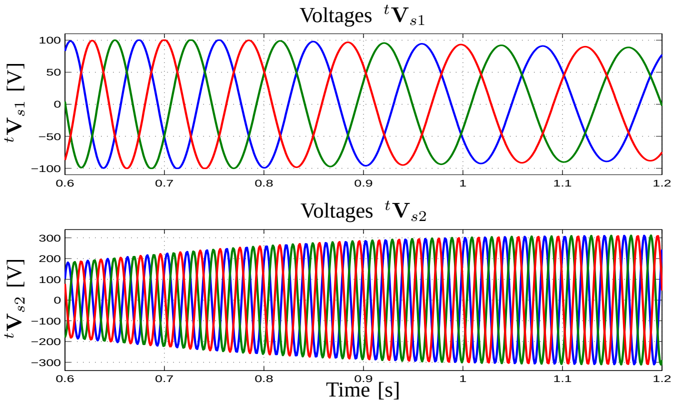

Figure 9. Stator voltages in the original reference frame Σ_t.

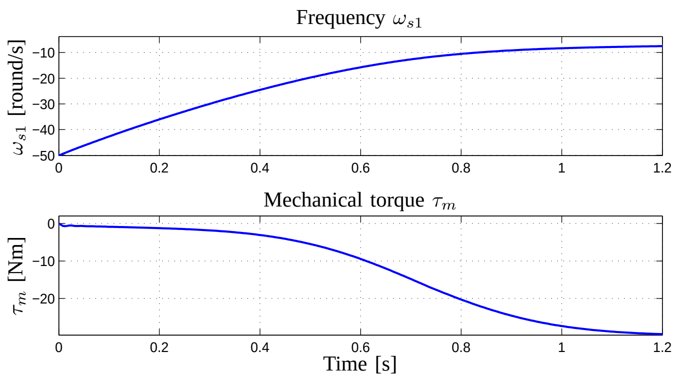

Figure 10. Frequency ω_{s1} and mechanical torque τ_m.

the corresponding model is very simple and compact, clearly showing the power internal structure of the system. A state space transformation has been used to refer the dynamic equations to a rotating reference frame. An Indirect Rotor Field-Oriented control has been implemented for the M_1 motor, that imposes a speed reference ω_m^{ref} in order to keep the grid voltage frequency ω_{s2} constant, by modulating the frequency

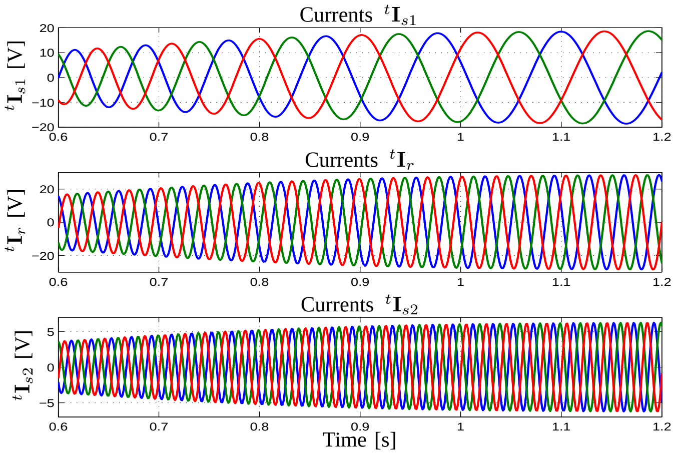

Figure 11. Stator and rotor currents in the original reference frame Σ_t.

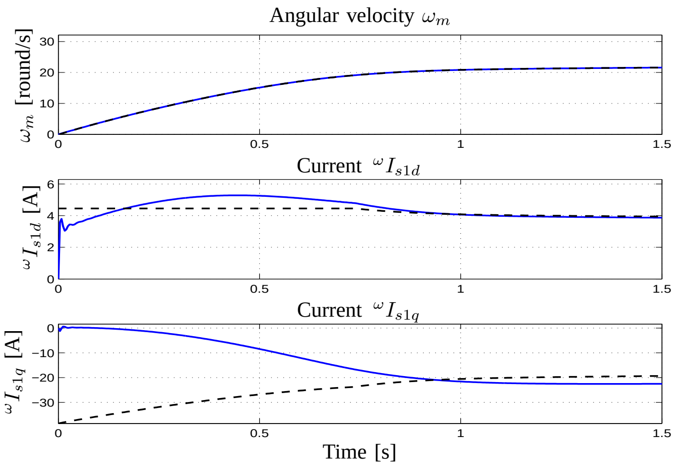

Figure 12. Actual (solid blue) and desired (dotted black) angular velocity and stator current dq components in the reference frame Σ_ω.

ω_{s1} of the input voltage vector ${}^t\mathbf{V}_{s1}$. Some simulation results have been reported to show the effectiveness of the realized model and of the implemented control.

References

[1] S. Kato, N. Hoshi, K. Oguchi, *Small-scale hydropower*, IEEE Industry Applications Magazine, Vol. 9, No. 4, pp. 32-38, July-Aug. 2003.

[2] N. Patin, E. Monmasson, J.-P. Louis, *Analysis and control of a cascaded doubly-fed induction generator*, Industrial Electronics Society, 2005. IECON 2005. 31st Annual Conference of IEEE 6-10 Nov. 2005.

[3] N. Patin, E. Monmasson, J.-P. Louis, *Modelling and Control of a Cascaded Doubly-Fed Induction Generator based on Dynamical Equivalent Circuits*, Electrimacs'08, 8-11 June 2008, Québec, Canada.

[4] M. Adamowicz, R. Strzelecki, D. Wojciechowski, *Steady State Analysis of Twin Stator Cascaded Doubly Fed Induction Generator*, Compatibility in Power Electronics, 2007. CPE '07, pp. 1-5, May 29 2007-June 1 2007.

[5] R. Zanasi, *Power Oriented Modelling of Dynamical System for Simulation*, IMACS Symp. on Modelling and Control of Technological System, Lille, France, May 1991.

[6] R. Zanasi, F. Grossi, G. Azzone, *The POG technique for Modeling Multi-phase Asynchronous Motors*, 5th IEEE International Conference on Mechatronics, Málaga, Spain, April 14-17, 2009.

[7] R. Zanasi, F. Grossi, G. Azzone, *Dynamic Behavior of Multi-phase Asynchronous Motors*, 10th European Control Conference, 23-26 August 2009, Budapest, Hungary.

[8] W. Leonhard, *Control of Electrical Drives*, 3rd Edition 2001, Springer-Verlag Berlin Heidelberg NewYork, ISBN 3-540-41820-2.